KARYA ILHAM PUBLISHING
CONNECTING MINDS, BRIDGING IDEAS, INSPIRING READERS

Advances in Fluid, Heat and Materials Engineering

Journal homepage:
https://karyailham.com.my/index.php/afhme/index
ISSN: 3083-8134

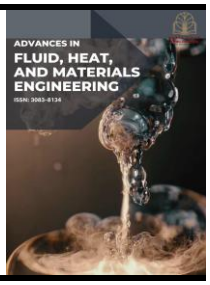

Numerical Prediction of Flow Characteristics in the Various Diameters of Serpentine Pipe

Abdul Rahman Abd Majid[1,*]

[1] Department of Mechanical Engineering, Faculty of Mechanical Engineering and Manufacturing, Universiti Tun Hussein Onn Malaysia, 86400 Batu Pahat, Johor, Malaysia

ARTICLE INFO

Article history:
Received 10 June 2025
Received in revised form 20 July 2025
Accepted 26 July 2025
Available online 29 September 2025

Keywords:
Serpentine pipe flow; computational flow dynamic; flow separation; secondary flow; pressure distribution; velocity profiles; turbulence intensity

ABSTRACT

The study on water flow inside serpentine pipes was conducted using Computational Fluid Dynamics (CFD) simulations with ANSYS Fluent software. The serpentine pipes, characterized by multiple bends and curves, influence fluid motion and pressure loss, which are critical for applications in cooling, heating, and fluid transport systems. The investigation focused on how varying pipe diameters of 1.5 cm, 2.0 cm, and 2.5 cm affect turbulent water flow while maintaining the same pipe geometry. The pipe design included repeated 180-degree bends connected by straight sections to capture curvature effects such as swirling flows known as Dean vortices. The RNG k-ε turbulence model was employed to accurately simulate these complex flow patterns. Mesh quality and grid independence tests were performed to ensure the reliability of the results. Findings revealed that smaller pipe diameters induced stronger swirling flows, and higher pressure drops due to tighter bends, whereas larger diameters resulted in smoother flow and reduced pressure loss. The turbulence model used was effective in capturing these flow behaviour's, validating its appropriateness for this type of analysis. In conclusion, pipe diameter was found to significantly influence flow patterns and pressure losses in serpentine pipes. CFD proved to be a valuable tool for predicting these effects, aiding engineers in designing more efficient piping systems by optimizing pipe size and shape to balance flow uniformity and energy loss. These insights are practical for enhancing thermal and fluid transport applications involving serpentine pipes.

1. Introduction

The aim of this study is to investigate how fluid flows behave inside serpentine pipes by using Computational Fluid Dynamics (CFD). Understanding how the shape of these pipes with their multiple bends and curves impacts the way the fluid moves. The methodology in this study involves the simulation of turbulent water flow through serpentine pipes using ANSYS Fluent software. Three different pipe diameters 1.5 cm, 2.0 cm, and 2.5 cm are modelled while keeping the serpentine curvature and flow paths consistent throughout. The pipe geometry is designed with alternating 180-

[1*] *Corresponding author.*
E-mail address: rahman.majid11@gmail.com

https://doi.org/10.37934/afhme.6.1.3949a

degree bends connected by straight sections allowing the repeated curvature effects such as the formation of secondary flows like Dean vortices, to be captured. The simulation process includes the creation of geometry, generation of the mesh, setting of boundary conditions, configuration of the solver, and conducting a grid independence test to ensure that the mesh size does not affect the results.

Radzai *et al.,* [1] was shown that serpentine designs can result in higher pressure drops, which may reduce cooling efficiency in radiant panels. Insights into laminar flow and heat transfer in mini channels were provided by Corti *et al*., [2] highlighting the valuable role of CFD in improving thermal system designs. The significance of multiphase flow behavior in U-bends was emphasized by Kazi *et al*., [3] The amount of gas and liquid inside the pipe is important for improving heat related systems while erosion issues in bends handling slurry flows were addressed by Wu *et al*., [4]. Huang and Le *et al*., [5] show that the twists and curves in the nozzle can lead to uneven stress distribution that helps in designed nozzles stay strong and reliable in tough conditions. Park *et al*., [6] discovered that when the Reynolds number goes up, the flow inside pipes becomes more even. Mosa *et al*., [7] highlights how different channel layouts can make cooling more efficient by improving how heat is transferred across the panel. Adegoke *et al*., [8] found that instability can occur in pipes carrying pulsating two-phase flow.

The impact of erosion and corrosion on nozzle designs was investigated by Khan *et al*., [9] illustrated that both material selection and nozzle geometry play a crucial role in preventing failures. The use of serpentine pipes in solar applications was explored by Ramlee *et al*., [10] that the design of pipes plays a key role in boosting thermal efficiency. Turbulent pipe flow was investigated by Pirozzoli *et al*., [11] found that at high Reynolds numbers, turbulence has a strong effect on the near-wall layers, indicating that the flow dynamics close to the pipe wall can significantly shape the overall behaviours of turbulence throughout the pipe.

The effects of secondary currents on turbulence in partially filled pipes were explored by Liu *et al*., [12] found that turbulence tends to concentrate near the pipe walls. Their study confirmed earlier observations that turbulence starts in the buffer and viscous layers close to the wall, while farther away from the wall, the turbulence becomes more uniform and isotropic. The transition from laminar to turbulent flow in pipes was investigated by Yokoo *et al*.,[13] found that distinct turbulence characteristics appear at a critical Reynolds number of around 3000. Kurevija *et al*., [14] shown that these designs lead to greater heat transfer between the fluid and the pipe material. Computational fluid dynamics (CFD) has been emphasized by Ahn *et al*., [15] with its ability to drive innovation recognized through the detailed insights it provides-insights that often go beyond what traditional experimental methods can offer. Sanavio and Sauro [16] recognized that despite current computational challenges, quantum approaches could significantly advance CFD simulations. Quantum algorithms allow much faster and more detailed simulations than traditional methods, opening new possibilities for solving complex fluid dynamics problems.

A range of numerical techniques in CFD has been reviewed by Nanda *et al*., [17] usefulness across different scales from large ocean currents to tiny blood vessels has been demonstrated. The integration of machine learning with CFD has been discussed by Cornfield and Karen [18] shown that this approach streamlines design processes by improving computational speed. By combining advanced algorithms with CFD simulations, faster and more efficient analysis possible, allowing for quicker optimization and innovation in engineering applications. Bhatti *et al*., [19] provided a review of recent trends in CFD emphasizing its foundational principles such as mass and energy conservation. Zhang *et al*., [20] proven that these improvements make simulations more accurate, especially when modelling complex shapes by using adaptive and mesh free methods, the process of

creating meshes has been made easier and better suited for capturing detailed flow features in challenging geometries.

2. Methodology

2.1 Geometry

The geometry of the serpentine pipe was created in ANSYS 2024 R2 Design Modeler (Canonsburg, Pennsylvania, United States), with the total axial length set at 95 cm for all cases. Three different models were built to study how changing the pipe diameter affects turbulent flow, while keeping the same serpentine curvature and flow path (Figure 1). Each model had an internal diameter of either 1.5 cm, 2.0 cm, or 2.5 cm. The serpentine profile was formed by connecting a series of alternating 180-degree bends with straight sections, ensuring repeated curvature along the flow direction. Geometrical constraints were applied so that the bend radius and spacing between turns remained uniform, allowing for direct comparison between the cases. All geometries were carefully checked for continuity before moving on to mesh generation.

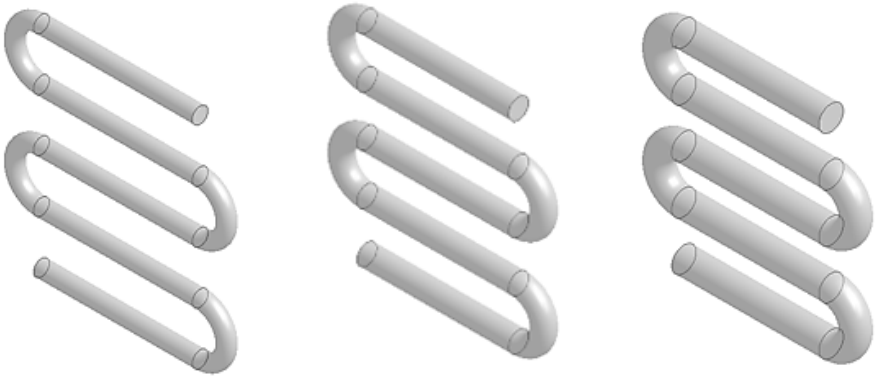

(a) (b) (c)

Fig. 1. The geometry of serpentine pipe in various diameter (a) 1.5 cm (b) 2.0 cm (c) 2.5 cm

2.2 Meshing

Mesh generation for the serpentine pipe geometries was performed in ANSYS Meshing, where a structured hexahedral-dominant mesh was used wherever the geometry allowed, and unstructured tetrahedral elements were applied in highly curved regions to better fit the complete pipe shape (Figure 2). To ensure mesh quality and reliable results, three different mesh densities were created for each pipe diameter as shown in Table 1, and a Grid Independence Test was carried out to confirm that the simulation outcomes were not affected by mesh resolution.

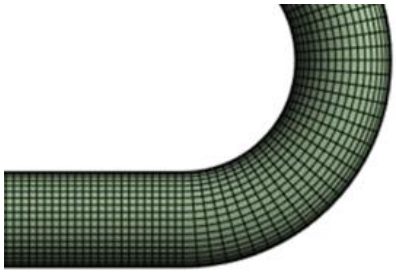

Fig. 2. The generate mesh

Table 1
Grid independence test (GIT) variables

1.5 cm diameter		2 cm diameter		2.5 diameter	
Element size (m)	Nodes	Element size (m)	Nodes	Element size (m)	Nodes
0.002	68,666	0.002	97,344	0.002	164,076
0.0016	114,145	0.0016	222,123	0.0016	325,458
0.0012	324,008	0.0012	477,692	0.0012	703,500

2.3 Governing Equation

The flow of water through the serpentine pipe was governed by the fundamental equations of fluid dynamics, specifically the continuity equation for mass conservation and the Navier-Stokes equations for momentum conservation. Due to the turbulent nature of the flow and the complex geometry, these equations were solved using Reynolds-Averaged Navier-Stokes (RANS) formulations in combination with an appropriate turbulence model. There are formula of continuity and Navier-Stokes momentum equations

$$\nabla.\vec{V} = 0 \tag{1}$$

$$\rho\left(\frac{\partial\vec{V}}{\partial t} + \vec{V}.\nabla\vec{V}\right) = -\nabla p + \mu\nabla^2\vec{V} + \vec{F} \tag{2}$$

2.4 Boundary Conditions

Once the mesh generation was completed, the boundary conditions for all the serpentine pipe geometries were carefully set up within ANSYS Fluent. At the pipe inlet, a velocity inlet condition was applied, with three different velocities $0.297\,\frac{\mathrm{m}}{\mathrm{s}}, 0.397\,\frac{\mathrm{m}}{\mathrm{s}}, \text{and } 0.497\ \mathrm{m/s}$ used in separate simulation cases. These specific velocities were chosen to maintain a Reynolds number close to 4338 across all pipe diameters $1.5\ \mathrm{cm}, 2.0\ \mathrm{cm}, \text{and } 2.5\ \mathrm{cm}$, ensuring that turbulent flow conditions were consistently represented throughout the study.

At the outlet, a pressure outlet condition was specified, with the gauge pressure set to 0 Pa, allowing the flow to exit the domain naturally without artificial restrictions. The internal surfaces of the serpentine pipes were treated as no-slip walls, meaning the fluid velocity at the pipe walls was set to zero. To model the turbulent nature of the flow, a turbulence model suitable for internal flows with curvature effects was selected the k-ω SST model. The same boundary condition setup was applied consistently across all mesh densities and pipe diameters. This approach ensured that any differences observed in the simulation results could be attributed solely to changes in pipe diameter or inlet velocity.

2.5 Analysis of Serpentine Pipe

After the simulations reached convergence, the results were examined using ANSYS Fluent's built in visualization and data extraction tools. Flow features were visualized by generating velocity, pressure, and turbulence intensity contours, which helped to show how the flow developed along the serpentine pipe. Streamline plots were also created, making it possible to see secondary flow structures and vortices caused by the pipe's curvature-features that are typical in serpentine channels under turbulent conditions. To better understand the flow, velocity profiles were taken at

specific cross-sections after major bends and along straight sections of the pipe. The static pressure at the inlet and outlet was recorded to calculate the overall pressure drop for each case, allowing the effects of inlet velocity and pipe diameter to be compared. Turbulence quantities such as turbulent kinetic energy and vorticity were analysed to assess how diameter and curvature influenced flow instability.

3. Results

3.1 Grid Independence Test (GIT)

To ensure the CFD simulation results were accurate, a Grid Independence Test (GIT) was performed. For each pipe diameter 1.5 cm, 2.0 cm, and 2.5 cm, three different mesh sizes 0.002 m, 0.0016 m, and 0.0012 m were tested to evaluate how mesh density influenced the outcomes. The static pressure drops and velocity magnitude along the serpentine pipe were closely tracked. By comparing results across mesh sizes, it was confirmed that finer meshes did not significantly alter the pressure or velocity predictions, ensuring reliable and consistent simulations. This step helped validate the chosen mesh resolution was sufficient to capture critical flow features without unnecessary computational cost.

3.1.1 Velocity distribution

As the mesh was refined from 0.002 m to 0.0012 m, the velocity profiles for all three pipe diameters became more detailed. With the coarser mesh 0.002 m, the velocity contours appeared smoother, and the gradients near the walls and curved sections were less distinct. When the mesh density was increased to medium 0.0016 m and fine 0.0012 m, sharper changes and more accurate boundary layer behaviours were captured. However, the difference in velocity magnitude between the medium and fine meshes was very small, indicating that the velocity field had essentially converged, as shown in Figure 3.

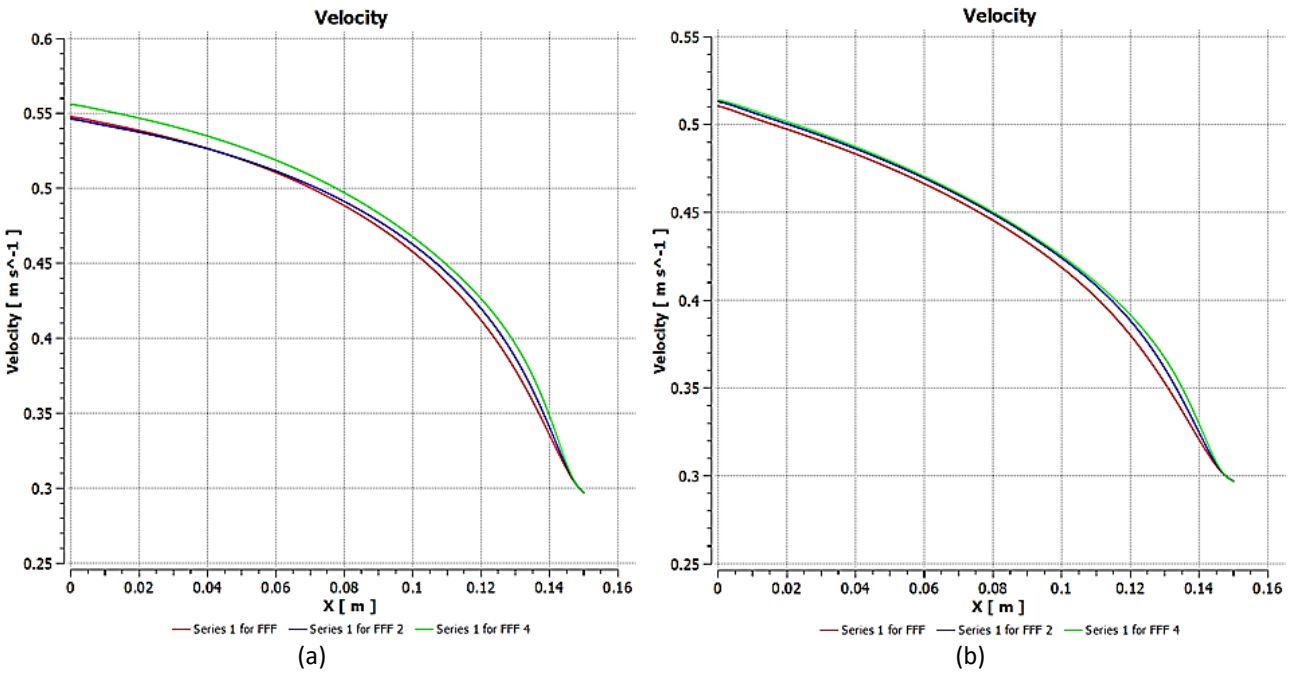

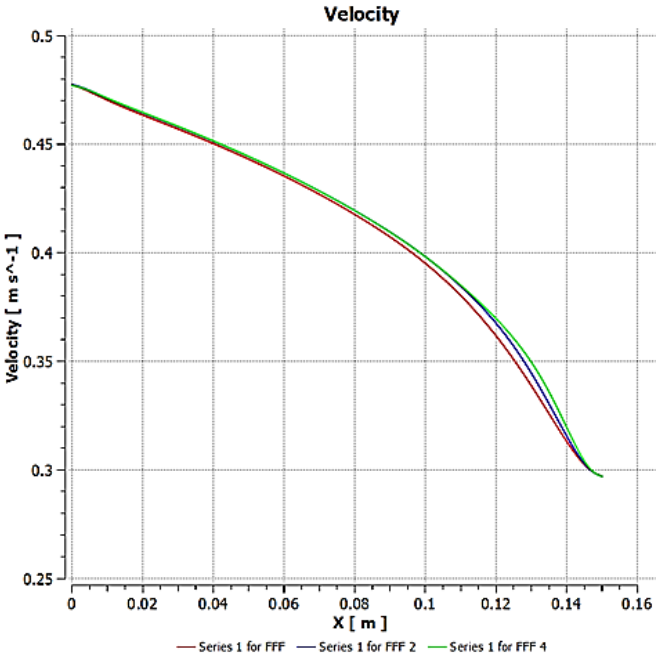

(c)

Fig. 3. The GIT chart of velocity (a) Diameter 1.5 cm (b) Diameter 2.0 cm (c) Diameter 2.5 cm

3.1.2 Pressure distribution

The static pressure results showed a similar trend. As the mesh was refined, the pressure drops along the pipe increased slightly, especially when moving from the course to the medium mesh. This happened because the finer mesh better captured the pressure changes in the curved sections, were flow separation and recirculation cause energy losses. However, between the medium and fine meshes, the pressure drops values remained nearly the same, with only minor differences observed, as shown in Figure 4.

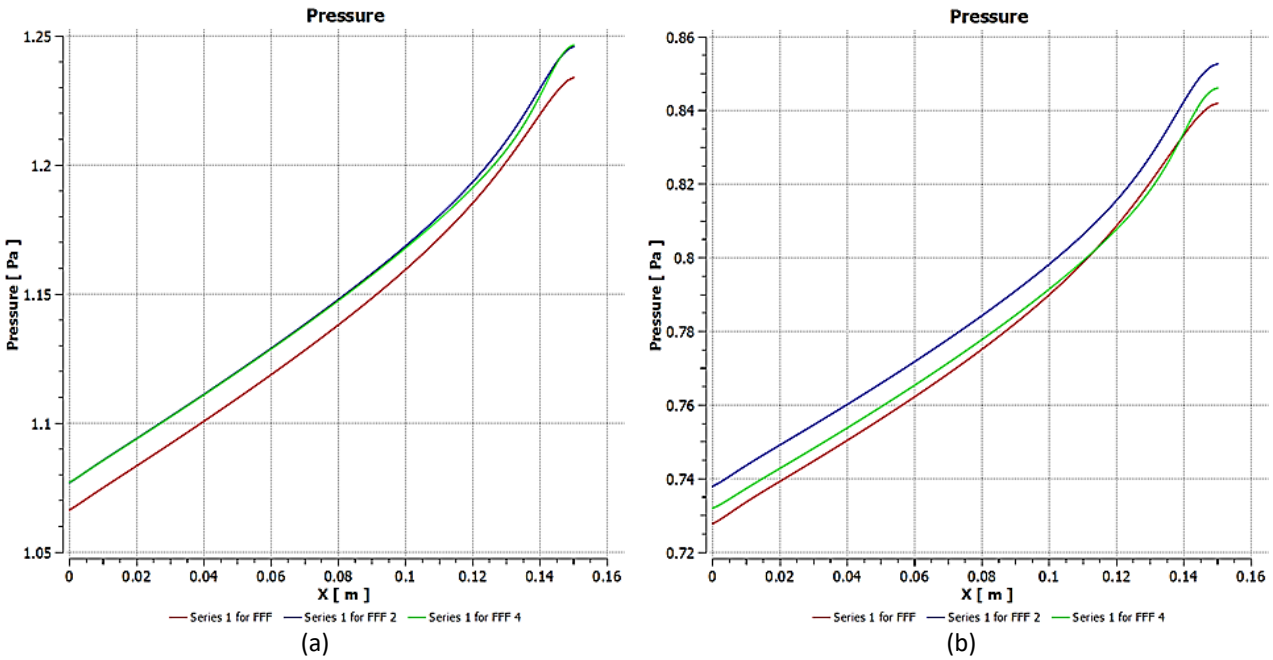

(a) (b)

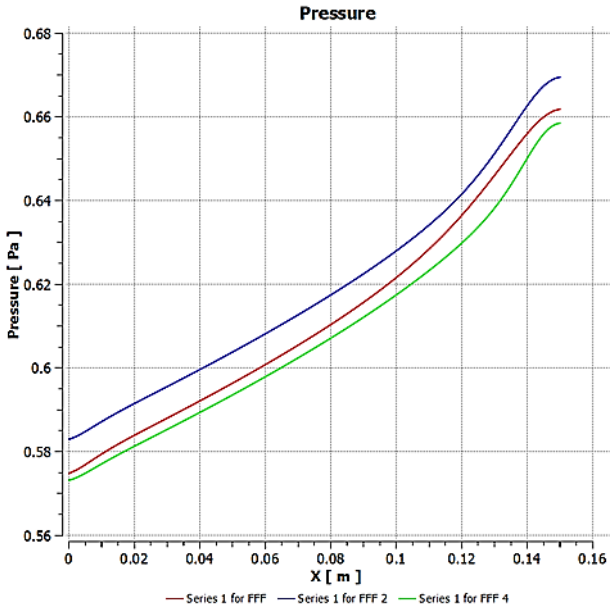

(c)

Fig. 4. The GIT chart of pressure (a) Diameter 1.5 cm (b) Diameter 2.0 cm (c) Diameter 2.5 cm

3.2 Contour Velocity

Velocity contours were used to visualize how the fluid moves through the serpentine pipe across different diameters and inlet velocities. These contour plots revealed the speed of the fluid at various points within the pipe. Observed that higher fluid velocities appeared along the inner side of each bend, while lower velocities were found on the outer side. This happens because the pipe's curved shape causes the fluid to accelerate and decelerate in different areas. As the inlet velocity increased, the fluid flow faster and the velocity gradients near the pipe walls became steeper, indicating stronger shear forces, as shown in Figures 5 to 7.

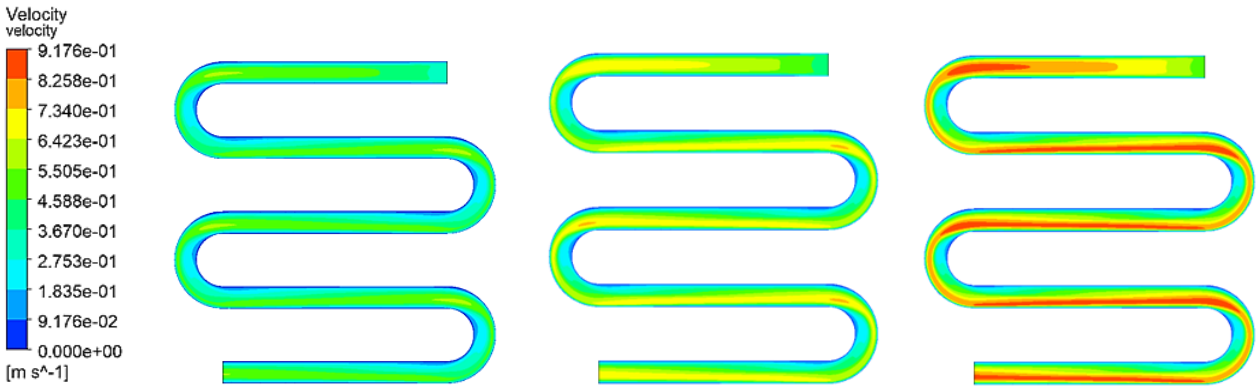

(a) (b) (c)

Fig. 5. The velocity contour diameter 1.5 cm in different velocity (a) 0.297 m⁄s (b) 0.397 m⁄s (c) 0.397 m⁄s

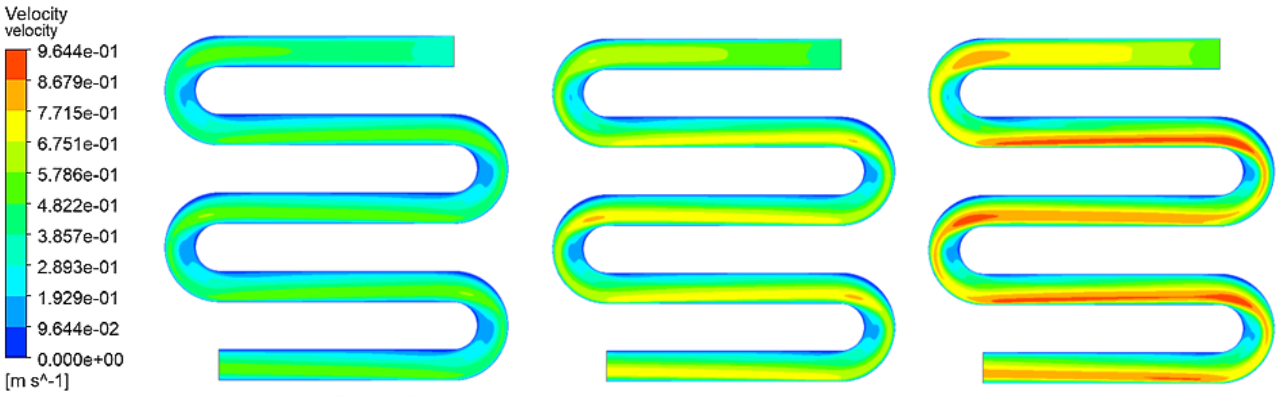

(a) (b) (c)

Fig. 6. The velocity contour diameter 2.0 cm in different velocity (a) 0.297 m⁄s (b) 0.397 m⁄s (c) 0.397 m⁄s

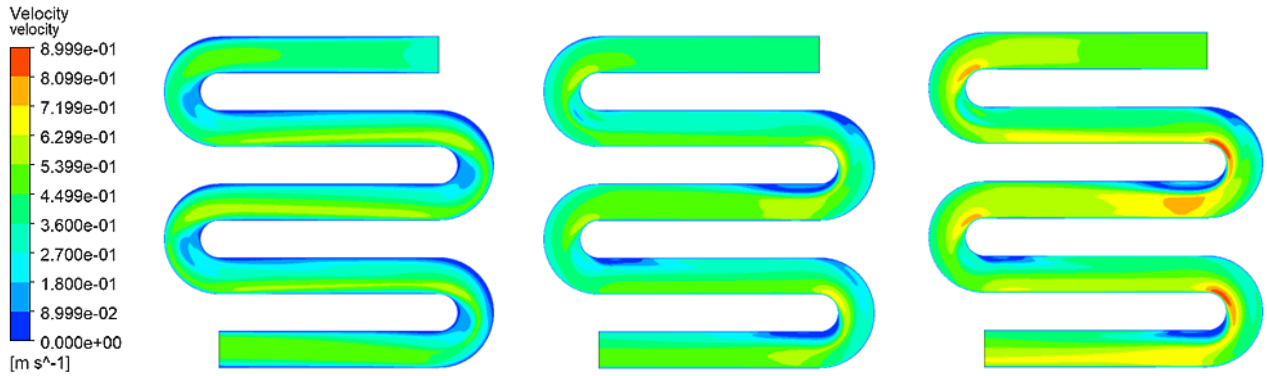

(a) (b) (c)

Fig. 7. The velocity contour diameter 2.5 cm in different velocity (a) Velocity 0.297 m⁄s (b) Velocity 0.397 m⁄s (c) Velocity 0.397 m⁄s

3.3 Contour Pressure

The pressure contour from the simulation reveals a clear area of high pressure at the front face of the object, marking the stagnation point where the incoming fluid flow hits the surface directly. This area is shown as a red zone in the contour. As the fluid moves around the shape, the pressure gradually drops along the sides, shifting from green to blue shades. The lowest pressure is found at the rear of the object, where the flow separates and creates a wake zone, represented by the blue colour (Figures 8 to 10).

(a) (b) (c)

Fig. 8. The pressure contour diameter 1.5 cm in different velocity (a) 0.297 m⁄s (b) 0.397 m⁄s (c) 0.497 m⁄s

(a) (b) (c)

Fig. 9. The pressure contour diameter 2.0 cm in different velocity (a) 0.297 m⁄s (b) 0.397 m⁄s (c) 0.497 m⁄s

(a) (b) (c)

Fig. 10. The pressure contour diameter 2.5 cm in different velocity (a) 0.297 m⁄s (b) 0.397 m⁄s (c) 0.497 m⁄s

3.4 Contour Turbulence Kinetic Energy

The turbulence kinetic energy (TKE) contour highlights areas where turbulence is strongest due to the interaction between the fluid flow and the model's surface. From the simulation, the highest TKE values appear at the rear of the object, where flow separation and vortex shedding occur. This area is shown in yellow to red on the contour plot. Moderate turbulence levels are also found along the edges of the body, where shear layers develop because of velocity differences. In contrast, the front of the object experiences relatively low TKE, as the flow remains attached and more uniform there. This TKE distribution is typical for external flow around a bluff body, with most turbulent activity concentrated in the wake region, indicating increased mixing and energy loss in that area.

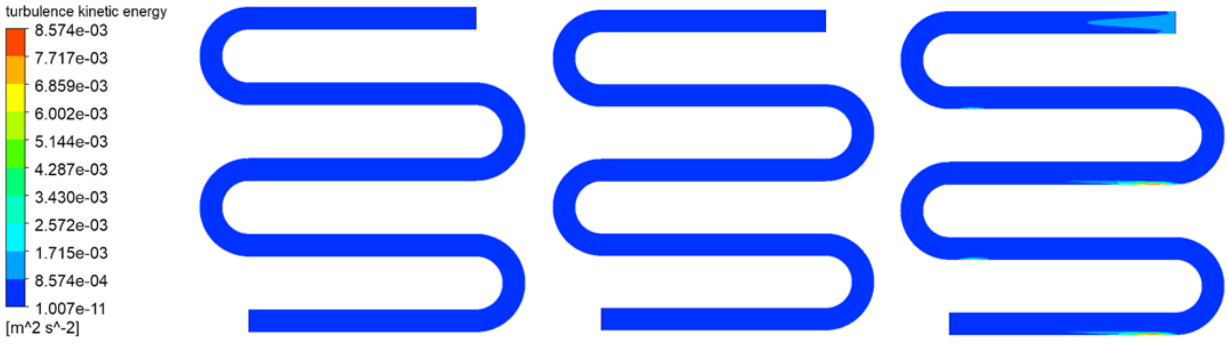

(a) (b) (c)

Fig. 11. The turbulence kinetic energy contour diameter 1.5 cm in various velocity (a) 0.297 m⁄s (b) 0.397 m⁄s (c) 0.497 m⁄s

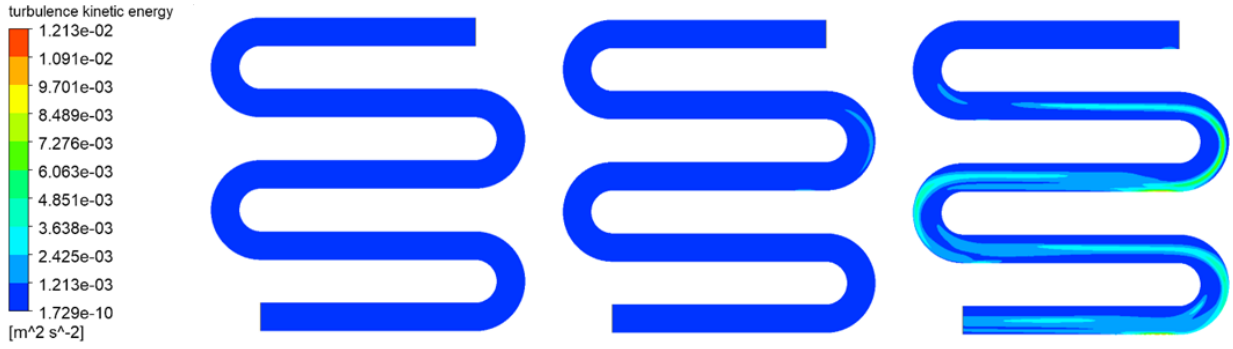

Fig. 12. The turbulence kinetic energy contour diameter 2.0 cm in various velocity (a) 0.297 m⁄s (b) 0.397 m⁄s (c) 0.497 m⁄s

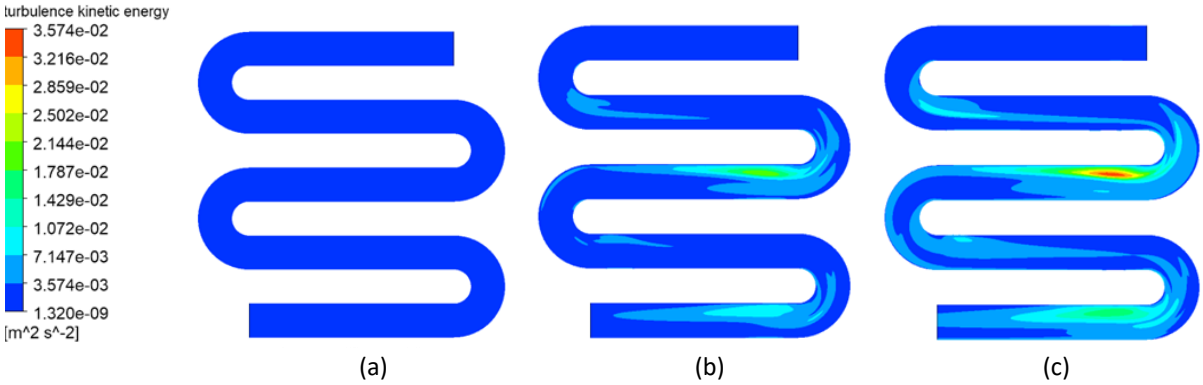

Fig. 12. The turbulence kinetic energy contour diameter 2.5 cm in various velocity (a) 0.297m⁄s (b) 0.397m⁄s (c) 0.497m⁄s

4. Conclusions

This study demonstrated that Computational Fluid Dynamics (CFD) is a powerful and reliable tool for analysing complex fluid behaviours in serpentine pipes. Turbulent water flow through pipes of different diameters but identical serpentine geometry was simulated, and it was found that flow patterns, pressure drop, and the formation of secondary flows such as Dean vortices are significantly affected by pipe diameter. Stronger secondary flows and higher-pressure losses were observed in smaller diameters, while smoother flow with reduced energy loss was exhibited by larger diameters. The importance of careful pipe design in engineering applications, where efficient fluid transport and heat transfer are critical, has been highlighted by these results.

References

[1] Radzai, Mohammad Hakim Mohd, Chong Tak Yaw, Chin Wai Lim, Siaw Paw Koh, and Nur Amirani Ahmad. "Numerical analysis on the performance of a radiant cooling panel with serpentine-based design." *Energies* 14, no. 16 (2021): 4744. https://doi.org/10.3390/en14164744

[2] Corti, M., C. LA Terra, C. Fanciulli, and A. Niro. "Convective heat transfer CFD analysis of forced flow through a half-stadium serpentine mini-channel at low Reynolds number." In *Journal of Physics: Conference Series*, vol. 2177, no. 1, p. 012011. IOP Publishing, 2022. https://doi.org/10.1088/1742-6596/2177/1/012011

[3] Kazi, Junichiro, Jumpei Fukuma, Ryo Kurimoto, Kosuke Hayashi, and Akio Tomiyama. "Void fractions in U-bends of a serpentine tube." *Multiphase Science and Technology* 34, no. 4 (2022). https://doi.org/1615/MultScienTechn.2022044148

[4] Wu, Boqiang. "CFD-DEM based wind-deposited sand high concentration slurry pipe transport characteristics and erosion study." In *Journal of Physics: Conference Series*, vol. 2280, no. 1, p. 012041. IOP Publishing, 2022. https://doi.org/10.1088/1742-6596/2280/1/012041

[5] Huang, Sheng, and Le Rong. "Parametric analysis of the shear lag effect in serpentine nozzles under fluid-thermal-solid coupling influence." In *Proceedings of Global Power and Propulsion Society* (2021). https://doi.org/10.33737/gpps21-tc-233

[6] Park, No-Suk, Sukmin Yoon, Woochang Jeong, and Yong-Wook Jeong. "Application of double piping theory to parallel-arrayed low-pressure membrane module header pipe and experimental verification of flow distribution evenness." *Membranes* 12, no. 7 (2022): 720. https://doi.org/10.3390/membranes12070720

[7] Mosa, Mohamed, Matthieu Labat, and Sylvie Lorente. "Constructal design of flow channels for radiant cooling panels." *International Journal of Thermal Sciences* 145 (2019): 106052. https://doi.org/10.1016/j.ijthermalsci.2019.106052

[8] Adegoke, Adeshina, Akin Fashanu, Olayinka Adewumi, and Ayowole Oyediran. "Nonlinear vibrations of a cantilevered pipe conveying pulsating two phase flow." *Research on Engineering Structure & Materials* (2019). https://doi.org/10.17515/resm2019.145me0902

[9] Khan, Rehan, Michał Wieczorowski, Darko Damjanović, Mohammad Rezaul Karim, and Ibrahim A. Alnaser. "Erosion–Corrosion failure analysis of a mild steel nozzle pipe in water–sand flow." *Materials* 16, no. 22 (2023): 7084. https://doi.org/10.3390/ma16227084

[10] Ramlee, Muhamad Fadhli, Adnan Ibrahim, Hasila Jarimi, Noorliyana Ramlee, and Ahmad Fazlizan. "Numerical evaluation of thermal performance of two-phased closed thermosyphon for solar applications." In *IOP Conference Series: Materials Science and Engineering*, vol. 1278, no. 1, p. 012008. IOP Publishing, 2023. https://doi.org/10.1088/1757-899X/1278/1/012008

[11] Pirozzoli, Sergio, Joshua Romero, Massimiliano Fatica, Roberto Verzicco, and Paolo Orlandi. "One-point statistics for turbulent pipe flow up to." *Journal of Fluid Mechanics* 926 (2021): A28. https://doi.org/10.1017/jfm.2021.727

[12] Liu, Yan, T. Stoesser, and H. Fang. "Effect of secondary currents on the flow and turbulence in partially filled pipes." *Journal of Fluid Mechanics* 938 (2022): A16. https://doi.org/10.1017/jfm.2022.141

[13] Yokoo, Hikaru, Mizuki Yamamoto, Takumi Matsumoto, Takahiro Yamada, and Takeshi Kanda. "Study of the reverse transition in pipe flow." *Scientific Reports* 13, no. 1 (2023): 12333. https://doi.org/10.21203/rs.3.rs-3008324/v1

[14] Kurevija, Tomislav, Adib Kalantar, Marija Macenić, and Josipa Hranić. "Investigation of steady-state heat extraction rates for different borehole heat exchanger configurations from the aspect of implementation of new turbocollector™ pipe system design." energies 12, no. 8 (2019): 1504. https://doi.org/10.3390/en12081504

[15] Ahn, Joon. "Special Issue on “Advances and applications in computational fluid dynamics”." *Applied Sciences* 14, no. 23 (2024): 11060. https://doi.org/10.3390/app142311060

[16] Sanavio, Claudio, and Sauro Succi. "Quantum computing for simulation of fluid dynamics." arXiv preprint arXiv:2404.01302 (2024). https://doi.org/10.5772/intechopen.1005242

[17] Nanda, Dipika. Fluid dynamics: Modeling and simulation. *Pharma Innovation* 8, no 1 (2019), 796-799. https://doi.org/10.22271/tpi.2019.v8.i1m.25481

[18] Cornfield, Matthew, and Karen Bradshaw. "An exploration of flow control using machine learning and computational fluid dynamics." In *International Conference on Artificial Intelligence and its Applications*, pp. 120-127. 2023. https://doi.org/10.59200/ICARTI.2023.017

[19] Bhatti, Muhammad Mubashir, M. Marin, Ahmed Zeeshan, and Sara I. Abdelsalam. "Recent trends in computational fluid dynamics." *Frontiers in Physics* 8 (2020): 593111. https://doi.org/10.3389/fphy.2020.593111

[20] Zhang, Haoxuan, Haisheng Li, Xiaoqun Wu, and Nan Li. "Surface structured quadrilateral mesh generation based on topology consistent-preserved patch segmentation." *International Journal for Numerical Methods in Engineering* 126, no. 1 (2025): e7644. https://doi.org/10.1002/nme.7644